Reduced-Order Compensation: Linear-Quadratic Reduction Versus Optimal Projection

S. W. Greeley* and D. C. Hyland†
Harris Corporation, Melbourne, Florida

Six methods for design of reduced-order compensation are compared using an example problem. The methods considered comprise five linear-quadratic reduction techniques, reviewed in a recent paper by Liu and Anderson, and the Optimal Projection theory as implemented via a simple homotopy solution algorithm. Design results obtained by the different methods for 42 different design cases are compared with respect to closed-loop stability and transient response characteristics. Of the linear-quadratic reduction procedures, two are found to offer distinctly superior performance. However, only the Optimal Projection method provided stable designs in *all* cases. Further details are given on the performance of the numerical algorithm for solving the optimal projection equations and the corresponding design results.

I. Introduction

THE design of reduced-order dynamic controllers for high-order systems is of considerable importance for applications involving large spacecraft and flexible flight systems. Hence, it is not surprising that extensive research has been devoted to this area. A recent paper by Liu and Anderson[1] subjected five reduced-order controller design methods to both theoretical and numerical comparison. The computational comparison was based upon an example problem considered by Enns.[2] The five methods compared in Ref. 1 are:

1) Method of Enns[2]: This method is a frequency-weighted, balanced realization technique applicable to either model or controller reduction.

2) Method of Glover[3]: This method uses the theory of Hankel norm optional approximation for controller reduction.

3) Davis and Skelton[4]: This is a modification of compensator reduction via balancing that covers the case of unstable controllers.

4) Yousuff and Skelton[5]: This is a further modification of balancing for handling stable or unstable controllers.

5) Liu and Anderson[1]: In place of using a balanced approximation of the compensator transfer function directly, this method approximates the component parts of a fractional representation of the compensator.

All of the above methods proceed by first obtaining the full-order LQG compensator design for a high-order state-space model and then reducing the dimension of this LQG compensator.

The present paper complements the results of Liu and Anderson by giving a numerical comparison (again using Enns' example) of methods 1–5 with a sixth method: 6) optimal projection (OP) equations,[6] reduced-order compensator design by direct solution of the necessary conditions for quadratically optimal fixed-order dynamic compensation.

Method 6, like methods 1–5, has been shown to have intimate connections with balancing ideas.[7] Moreover, the first step in one iterative method for solution of the OP equations is almost identical to method 4. Method 6 differs from the other methods, however, in that it does not reduce the order of a previously obtained LQG design but rather directly characterizes the quadratically optimal compensator of a given fixed-order. The OP equations constitute four coupled, modified Riccati and Lyapunov equations wherein the steps of regulator design, observer design, and order reduction are completely and inseparably intermingled.

The principal objective of this paper is to provide a numerical comparison of the six methods of controller-order reduction on the same example problem. We do not attempt, however, to provide a complete theoretical comparison of the various methods as this would be a paper by itself.

The organization of this paper is as follows. In Sec. II, we state the problem considered and review the OP design equations. Section III gives the computational algorithm used herein for OP design synthesis. Finally, Sec. IV sets forth the example problem of Enns and compares the results of all six methods obtained for this example.

II. Problem Statement and Review of OP Design Equations

Here we consider the linear, finite-dimensional, time-invariant system:

$$\dot{x} = Ax + Bu + w_1; \qquad x \in R^N$$
$$y = Cx + w_2; \qquad y \in R^P \tag{1}$$

where x is the plant state, A is the plant dynamics matrix, and B and C are control input and sensor output matrices, respectively. Where w_1 is white disturbance noise with intensity matrix $V_1 \geq 0$ and w_2 is observation noise with nonsingular intensity $V_2 > 0$.

The reduced-order compensation problem consists in designing a constant gain dynamic compensator of order $N_c < N$:

$$u = -Kq, \qquad u \in R^{\ell}$$
$$\dot{q} = A_c q + Fy; \qquad q \in R^{N_c} \tag{2}$$

Obviously, the heart of the design problem is the selection of the constant matrices K, F, and A_c.

Methods 1–6 all associate with the closed-loop system [Eqs. (1) and (2)] a steady-state quadratic performance index J:

$$J \triangleq \lim_{t_1 - t_0 \to \infty} \tilde{J}/|t_1 - t_0|$$
$$\tilde{J} \triangleq \int_{t_0}^{t_1} dt\, [x^T R_1 x + u^T R_2 u] \tag{3}$$
$$R_1 \geq 0, \quad R_2 > 0$$

Received May 20, 1987; revision received Sept. 29, 1987.

*Technical Staff, Control Systems Engineering Group, Government Aerospace Systems Division.

†Leader, Control Systems Engineering Group, Government Aerospace Systems Division.

Methods 1–5 first design an LQG compensator (select K, F, A_c to minimize J) and then reduce the order of the resulting N state compensator. Thus, in methods 1–5, the quadratic performance [Eq. (3)] is brought into play in the initial LQG design step, but a variety of balancing and Hankel norm approximation ideas are used for the subsequent compensator-order reduction step. In contrast, method 6 selects K, F, and A_c by addressing the quadratically optimal, fixed-order compensation problem, i.e., for N_c fixed (and $< N$) choose K, F, and A_c to minimize J. The OP design methodology proceeds by solving the first-order necessary conditions for this optimization problem using the new forms for the necessary conditions given in Ref. 6. The basic OP design equations reduce to four modified Lyapunov and Riccati equations all coupled by a projection of rank N_c. In general, these design equations produce compensators that cannot be obtained by reduction of an LQG compensator.[7]

Methods 1–5 have been reviewed extensively in Refs. 1–5 and will not be discussed in detail. Here we shall merely review the OP design equations to the extent needed to illustrate the solution algorithm used for this study.

To do this, a few preliminary results and notational conventions must be given. First we have Lemma 1[7]:

Lemma 1. Suppose $\hat{Q}\in R^{N\times N}$ and $\hat{P}\in R^{N\times N}$ are nonnegative definite and rank $(\hat{Q})$ = rank $(\hat{P})$ = rank $(\hat{Q}\hat{P})$. Then the product $\hat{Q}\hat{P}$ is semisimple (all Jordan blocks are of order unity) with real, nonnegative eigenvalues. Moreover, there exists a nonsingular $\Psi[\hat{Q},\hat{P}]$ such that:

$$\Psi^{-1}[\hat{Q},\hat{P}]\hat{Q}\hat{P}\Psi[\hat{Q},\hat{P}] = \Lambda^2 \tag{4a}$$

$$\Psi^{T}[\hat{Q},\hat{P}]\hat{P}\Psi[\hat{Q},\hat{P}] = \Lambda \tag{4b}$$

$$\Psi^{-1}[\hat{Q},\hat{P}]\hat{Q}\Psi^{-T}[\hat{Q},\hat{P}] = \Lambda \tag{4c}$$

where

$$\Lambda = \underset{k=1\ldots N}{\text{diag}} \{\Lambda_k\} \tag{5}$$

is the positive diagonal matrix of the square roots of the eigenvalues of $\hat{Q}\hat{P}$.

When for a given pair $\hat{Q}$ and $\hat{P}$, a $\Psi[\hat{Q},\hat{P}]$ exists such that Eq. (4) holds, $\hat{Q}$ and $\hat{P}$ are said to be contragradiently diagonalizable and balanced,[9] and $\Psi[\hat{Q},\hat{P}]$ constitutes a simultaneous contragradient transformation. Determination of such a transformation is the fundamental mathematical operation of balancing.

Furthermore, it is clear that the quantities

$$\Pi_k[\hat{Q},\hat{P}] \triangleq \Psi[\hat{Q},\hat{P}]E^{(k)}\Psi^{-1}[\hat{Q},\hat{P}]$$

$$E^{(k)}_{mn} = \begin{cases} 1;\ m=n=k \\ 0;\ \text{otherwise} \end{cases} \tag{6}$$

form a set of mutually disjoint unit rank projections, i.e.,

$$\Pi_k[\hat{Q},\hat{P}]\Pi_j[\hat{Q},\hat{P}] = \Pi_k[\hat{Q},\hat{P}]\delta_{kj} \tag{7}$$

Thus the sum of r distinct Π_k is itself a projection of rank r. Also $\hat{Q}\hat{P}$ can be alternatively expressed as

$$\hat{Q}\hat{P} = \sum_{k=1}^{n} \Pi[\hat{Q}\hat{P}]^2_k \tag{8}$$

By virtue of Eq. (8) and the usage in Ref. 10, we term $\Pi_k[\hat{Q}\hat{P}]$ the eigen-projection of $\hat{Q}\hat{P}$ associated with the k^{th} eigenvalue.

The above results and conventions, together with the following notations,

$$\Sigma \triangleq BR_2^{-1}B^T \tag{9a}$$

$$\bar{\Sigma} \triangleq C^T V_2^{-1} C \tag{9b}$$

$$\tau_\perp \triangleq I_n - \tau \tag{9c}$$

allow us to state the main result[6–8] upon which the OP reduced-order compensator design method is based.

Theorem 1. Consider the quadratically optimal, fixed-order compensation problem with $N_c \le N$ fixed.

Let nonnegative definite $Q, P, \hat{Q}, \hat{P} \in R^{N\times N}$ be determined as solutions to the following equations:

$$0 = AQ + QA^T + V_1 - Q\bar{\Sigma}Q + \tau_\perp Q\bar{\Sigma}Q\tau_\perp^T \tag{10a}$$

$$0 = A^T P + PA + R_1 - P\Sigma P + \tau_\perp^T P\Sigma P\tau_\perp \tag{10b}$$

$$0 = (A - \Sigma P)\hat{Q} + \hat{Q}(A - \Sigma P)^T + Q\bar{\Sigma}Q - \tau_\perp Q\bar{\Sigma}Q\tau_\perp^T \tag{10c}$$

$$0 = (A - Q\bar{\Sigma})^T\hat{P} + \hat{P}(A - Q\bar{\Sigma}) + P\Sigma P - \tau_\perp^T P\Sigma P\tau_\perp \tag{10d}$$

$$\tau = \sum_{K=1}^{N_c} \Pi_K[\hat{Q}\hat{P}] \tag{10e}$$

Then, with $\Gamma, G \in R^{N_c\times N}$ given by

$$\Gamma = [I_{N_c}, 0]\Psi^{-1}[\hat{Q},\hat{P}]$$

$$G = [I_{N_c}, 0]\Psi^{T}[\hat{Q},\hat{P}] \tag{11}$$

the gains

$$K = R_2^{-1}B^T P G^T$$

$$F = \Gamma Q C^T V_2^{-1} \tag{12}$$

$$A_c = \Gamma(A - Q\bar{\Sigma} - \Sigma P)G^T$$

determine an extremal of the performance index J.

As has been remarked in Ref. 8, the value of the performance index is unchanged by any transformation of the compensator state basis; in other words, for any nonsingular $S \in R^{N\times N}$

$$J(K,F,A_c) = J(KS, S^{-1}F, S^{-1}A_c S) \tag{13}$$

Furthermore, when $N_c = N$, τ is a rank N projection on R^N by virtue of Eq. (10e). Hence $\tau = I_N$ and $\tau_\perp = 0$, and Eqs. (10a) and (10b) become uncoupled Riccati equations for determination of Q and P. Also Γ and G become $\Psi^{-1}[\hat{Q},\hat{P}]$ and $\Psi^{T}[\hat{Q},\hat{P}]$. Finally, setting $S = \Psi^{-1}$ and using Eqs. (13) and (12), extremalizing gains are given by:

$$K = R_2^{-1}B^T P$$

$$F = QC^T V_2^{-1}$$

$$A_c = A - Q\bar{\Sigma} - \Sigma P \tag{14}$$

with Q and P given as solutions to the independent Riccati Eqs. (10a) and (10b), and with $\tau_\perp = 0$. Hence when $N_c = N$, the design Eqs. (10), (11), and (12) immediately reduce to the LQG design for a full-order compensator.

However, for $N_c < N$, Eqs. (10a–10e) are first-order necessary conditions and generally possess multiple solutions corresponding to multiple extremals that can exist. This matter was explored in Ref. 11 relative to the related quadratically optimal model reduction problem. Basically, Eq. (10e) tells us that the rank N_c projection τ, which defines the geometry of the fixed-order compensator, is the sum of N_c out of N eigenprojections of $\hat{Q}\hat{P}$. However, the necessary conditions do not tell us which N_c out of N eigenprojections are to be selected to secure a global minimum of J. Indeed for any possible selection of N_c eigenprojections out of N, Eqs. (10a–10e) may possess a solution corresponding to a local extremal. By virtue of Eq. (10e) and the notational conventions of Eqs. (4) and (8), the selection of N_c eigenprojections is defined (generically) by the manner in which the eigenvalues, Λ_k, are ordered. Recently, Richter[12] has applied topological degree theory to investigate the possible solution branches and the character of the associated extrema and has devised a homotopy solution algorithm which selects the Λ-ordering which homotopically converges to the global minimum.

For the example considered in this paper, we adopt the ordering convention:

$$\Lambda_1 \geq \Lambda_2 \geq \ldots \geq \Lambda_N \tag{15}$$

in constructing $\Psi[\hat{Q},\hat{P}]$. Equation (15) together with Eq. (10e) imply that τ is taken to be the sum of the N_c eigenprojections corresponding to the N_c largest eigenvalues of $\hat{Q}\hat{P}$. Generically, this choice leads to an unequivocal choice of one solution branch of Eq. (10) corresponding to a particular extremal.

Thus, the OP design method investigated here consists in solving Eq. (10) with convention Eq. (15) and then evaluating the gains according to Eq. (12). We apply a simple homotopy solution algorithm, described in Sec. III, to the example problem of Enns specified in Sec. IV and compare results with methods 1–5. A more advanced and efficient homotopy algorithm is given in Ref. 12.

III. An Algorithm for Solution of the OP Design Equations

As stated, the OP design method is to solve Eq. (10) [with stipulation Eq. (15)] for P, Q, $\hat{P}$, $\hat{Q}$, and then evaluate the gains using Eqs. (11) and (12). A logically distinct issue is precisely how Eqs. (10a–10e) are to be solved. Here we present an algorithm that has been used for some time and requires only a standard LQG software package for its implementation. For convenience, this same algorithm was employed to obtain the numerical results for method 6 presented in the next section.

The basic motivation of this algorithm is the observation that the four main equations, Eqs. (10a–10d), are coupled only via the terms involving $\tau_\perp$ on the right-hand sides. If these $\tau_\perp$ terms were deleted, then all five equations can be solved sequentially. Moreover, Eqs. (10a) and (10b) reduce to ordinary Riccati equations, and Eqs. (10c) and (10d) are Lyapunov equations. Likewise, under conditions in which $Q\Sigma Q$ and $P\Sigma P$ are "small" relative to the remaining terms (e.g., sufficiently small state-weighting and disturbance noise intensity and/or sufficiently large control weighting and observation noise intensity), the $\tau_\perp$ terms are typically found to have little effect. In this situation, the artiface of fixing an initial $\tau_\perp$ and then solving Eqs. (10a–10e) as ordinary Riccati and Lyapunov equations is likely to give a reasonable approximation to the true solution.

Since only the $\tau_\perp$ terms on the right of Eqs. (10a–10d) occasion most of the difficulties, it is necessary to somehow bring these terms into play gradually. There are two principal ways to do this. The first is an iterative relaxation approach; i.e., fix $\tau_\perp$, solve Eqs. (10a–10d) sequentially, then update τ using Eq. (10e), and repeat until convergence, in some sense, is achieved. The second method is a homotopy approach; i.e., multiply the $\tau_\perp$ terms by a scalar parameter, $\alpha\epsilon[0,1]$, then starting with $\alpha = 0$ and gradually incrementing α, solve Eqs. (10a–10e) repeatedly until $\alpha = 1$.

The algorithm used here consists of two iterative loops. The inner loop uses the relaxation approach and is embedded within an outer loop which implements the simple homotopy approach.

The inner loop follows the earlier computational scheme discussed in Ref. 7. The homotopy parameter $\alpha\epsilon[0,1]$ which multiplies the $\tau_\perp$ terms is held fixed within the inner loop and is only incremented on the outer loop. To initialize the inner loop, one first fixes τ equal to the previous iterate (or set $\tau = I_N$ when starting) and then solves Eqs. (10a–10d). Once new iterates for Q, P, $\hat{Q}$, $\hat{P}$ are obtained, τ is updated by determining the balancing transformation $\Psi[\hat{Q},\hat{P}]$. To enhance convergence of the modified Riccati equations, the updated τ is taken to be the weighted sum of all N eigenprojections; the first N_c eigenprojections are given unity weight while the r^{th} ($r > N_c$) eigenprojection is weighted by $\Lambda_r/\Lambda_{N_c} < 1$. As convergence proceeds, Λ_r/Λ_{N_c} approaches zero for all $r > N_c$, and the numerical rank of τ approaches N_c. The indicated convergence check tests the relative excess of the numerical rank of τ over N_c and terminates the inner loop iterations when this "rank excess" falls below tolerance ϵ. In these studies $\epsilon = 0.1$ is used. The inner loop is terminated when either this tolerance is achieved or when the prescribed number of iterations is exceeded.

When the convergence criterion is satisfied, the gains, K, F, and A_c, are computed using Eqs. (11) and (12), and the steady-state performance J is evaluated. Performance evaluation invokes no assumptions regarding the convergence and optimality of the solutions to Eqs. (10a–10e). Specifically, the values of K, F, and A_c resulting from application of Eq. (12) are accepted as they stand and are used to construct the system matrices of the augmented system with state vector $X^T = [x^T, q^T]$. Next the $N + N_c \times N + N_c$ Lyapunov equation for the second moment matrix of the augmented, closed-loop system is solved. Finally, J is evaluated as a linear function of various subblocks of the augmented system second moment matrix.

The outer loop implements the homotopy approach by incrementing the homotopy parameter α and controlling the increment step size. At the start, the inner loop is initialized by $\tau = I_N$. Otherwise, when α is incremented, the inner loop is initialized using P, Q, $\hat{P}$, $\hat{Q}$ and τ as obtained with the previous value of α. Taken to be 0 at the start, α is subsequently incremented by Δ. The default value of Δ is 0.1, although other desired values may be input. However, whenever the inner loop is terminated without achieving the convergence tolerance ϵ, the homotopy parameter increment Δ is halved. This provides simple control over the homotopy step size. The entire algorithm terminates when $\alpha = 1.0$. Alternatively, at the user's option, the algorithm can be terminated when the change of the performance index J over two successive outer loop iterations is sufficiently small, thus indicating acceptable convergence with respect to quadratic performance.

IV. A Design Example and Comparison of Results

We use the example problem given by Enns (Ref. 2) to compare methods 1–6. Results on this example obtained by use of methods 1–5 are discussed in Ref. 1. Here, we augment these results by considering method 6 and undertake an overall comparison.

The plant to be controlled in this example is a four-disk system and is linear, time-invariant, SISO, neutrally stable (with a double pole at the origin), and nonminimum phase and of eighth order. Numerical values of the matrices A, B, C, R_1, R_2, V_1, and V_2 defining this problem are given in Table 1.

For each of the methods 1–6, controllers of different reduced orders (from seventh to second order) were obtained for seven different values of the disturbance noise intensity parameter q_2:

$$q_2 = 0.01, 0.1, 1.0, 10, 100, 1000, 2000$$

Thus each method was used to obtain results on 42 different design cases.

Each of the six methods was originally devised according to a wide variety of different criterion for adequate performance of a reduced-order compensator design. Despite this wide disparity among the different aims and motivations of the several methods, there are at least three criteria that may be reasonably applied to judge the success of a reduced-order design: 1) closed-loop stability; 2) extent to which the reduced-order compensator impulse and step response match the full-order, LQG, compensator response; and 3) the closed-loop quadratic cost.

However, item 3 will not be considered since costs for methods 1–5 were not provided.[1] The comparison in item 2 examines the output $y(t)$ in response to an input injected into the closed loop at the controller input.

First, Table 2 summarizes the closed-loop stability properties of all design methods in all 42 cases. Generally, it is seen that all methods achieve a high rate of success in achieving closed-loop stability for the larger N_c values and small q_2. On the other hand, methods 1–5 experience greater difficulties for low values of N_c and, particularly, for large q_2. With respect to stability, the only qualitative distinction among the methods is that method 6 (optimal projection) produces stable design in all 42 design cases.

The trend toward increasing difficulty of the design with increasing disturbance noise intensity is highlighted by Table 3 which shows the percentage of closed-loop stable designs given by the different methods for the different values of q_2 and in total. That the fraction of stable designs declines with increasing q_2 is to be expected since larger disturbance noise intensity increases Q, thereby increasing observer gains to produce faster observers that are more sensitive to order reduction.

Overall, for this example problem, method 4 exhibits the smallest fraction of stable designs (with 24 unstable designs) and does not achieve any order reduction for $q_2 = 100$, 1000, 2000. Of the LQG reduction methods 1–5, methods 1 and 5 fare best, with only four unstable designs out of 42. As noted, optimal projection (method 6) yields stable designs in all cases.

To permit independent corroboration by interested readers of the OP design capabilities, we give numerical values of the compensator gains obtained by method 6 for a selection of the more difficult cases, namely: $q_2 = 2000$ and $N_c = 2, 3, 4$, and $N_c = 2$ and $q_2 = 0.01, 0.1, 1.0, 10, 100, 1000$.

Next, consider the accuracy with which the step and impulse responses of the various reduced-order compensator designs track the corresponding response of the full-order LQG design. These characteristics exhibit similar trends as noted with respect to closed-loop stability. For example, Fig. 1a shows a comparison of unit step responses for second-order compensator designs with a small value of q_2 (= 1.0). In this case, all methods are stable. However, methods 1 and 5 show distinctly superior tracking accuracy. For clarity, methods 1 and 5 are compared with method 6 in Fig. 1b. Here it is clear that method 5 is somewhat closer to the LQG response than method 1, although method 6 is closest of all.

Similar trends are seen in the comparisons of the impulse responses (for the same design case) in Fig. 2. Once again, of the LQG reduction methods (compared in Fig. 2a), methods 1 and 5 display significantly better agreement with the LQG re-

Table 1 Data matrices for the example problem of Enns[2]

$$A = \begin{bmatrix} -0.161 & 1 & 0 & 0 & 0 & 0 & 0 & 0 \\ -6.004 & 0 & 1 & 0 & 0 & 0 & 0 & 0 \\ -0.5822 & 0 & 0 & 1 & 0 & 0 & 0 & 0 \\ -9.9835 & 0 & 0 & 0 & 1 & 0 & 0 & 0 \\ -0.4073 & 0 & 0 & 0 & 0 & 1 & 0 & 0 \\ -3.982 & 0 & 0 & 0 & 0 & 0 & 1 & 0 \\ 0 & 0 & 0 & 0 & 0 & 0 & 0 & 1 \\ 0 & 0 & 0 & 0 & 0 & 0 & 0 & 0 \end{bmatrix}$$

$B^T = [0, 0, 0.0064, 0.00235, 0.0713, 1.0002, 0.1045, 0.9955]$

$C = [1, 0, 0, 0, 0, 0, 0, 0]$

$R_1 = (1.0 \times 10^{-6})H^T H$; $H = [0, 0, 0, 0, 0.55, 11, 1.32, 18.0]$

$R_2 = 1$

$V_1 = q_2 BB^T$ ($q_2 = [0.01, 2000.0]$)

$V_2 = 1$

Table 2 Stability of the reduced-order controller by different methods

Method	N_c \ $q_2 =$	0.01	0.1	1	10	100	1000	2000
Enns, 1	7	S	S	S	S	S	S	S
	6	S	S	S	S	S	S	S
	5	S	S	S	S	S	S	S
	4	S	S	S	S	S	S	U
	3	S	S	S	S	S	S	S
	2	S	S	S	S	U	U	U
Glover, 2	7	S	S	S	S	S	U	S
	6	S	S	S	S	U	U	U
	5	S	S	S	S	U	U	U
	4	S	S	S	S	U	U	U
	3	S	S	U	S	U	U	U
	2	S	U	S	U	S	U	U
Davis & Skelton, 3	7	S	U	U	S	S	S	S
	6	S	S	S	S	S	S	S
	5	S	U	S	S	S	U	U
	4	S	S	U	S	S	U	U
	3	U	U	U	U	U	U	U
	2	S	U	S	U	U	U	U
Yousuff & Skelton, 4	7	S	S	S	S	U	U	U
	6	S	S	S	S	U	U	U
	5	S	S	S	U	U	U	U
	4	S	S	S	U	U	U	U
	3	S	U	U	U	U	U	U
	2	S	S	S	U	U	U	U
Liu & Anderson, 5	7	S	S	S	S	S	S	U
	6	S	S	S	S	S	S	U
	5	S	S	S	S	S	S	S
	4	S	S	S	S	S	S	S
	3	S	S	S	S	S	U	U
	2	S	S	S	S	S	S	S
Optimal Projection, 6	7	S	S	S	S	S	S	S
	6	S	S	S	S	S	S	S
	5	S	S	S	S	S	S	S
	4	S	S	S	S	S	S	S
	3	S	S	S	S	S	S	S
	2	S	S	S	S	S	S	S

S: The closed-loop system is stable. U: The system is unstable.

Table 3 Percentage of stable designs given by the different methods

Method \ $q_2 =$	0.01	0.1	1	10	100	1000	2000	Total % for all cases
Enns[1]	100	100	100	100	83.3	83.3	66.7	90.5
Glover[2]	100	83.3	83.3	83.3	33.3	0	16.7	57.1
Davis & Skelton[3]	83.3	33.3	50.0	66.7	66.7	33.3	33.3	52.4
Yousuff & Skelton[4]	100	83.3	83.3	33.3	0	0	0	42.9
Liu & Anderson[5]	100	100	100	100	100	83.3	50.0	90.5
Optimal Projection[6]	100	100	100	100	100	100	100	100.0

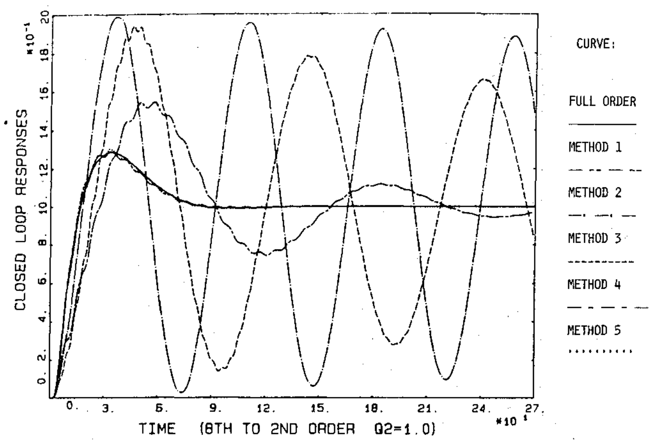

Fig. 1a **Comparison of unit step responses of second-order compensators given by methods 1–5 with full-order design (small q_2).**

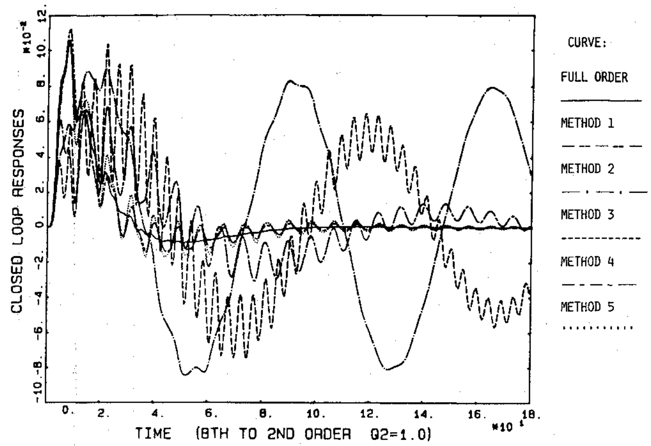

Fig. 2a **Comparison of impulse responses of second-order compensators given by methods 1–5 with full-order design (small q_2).**

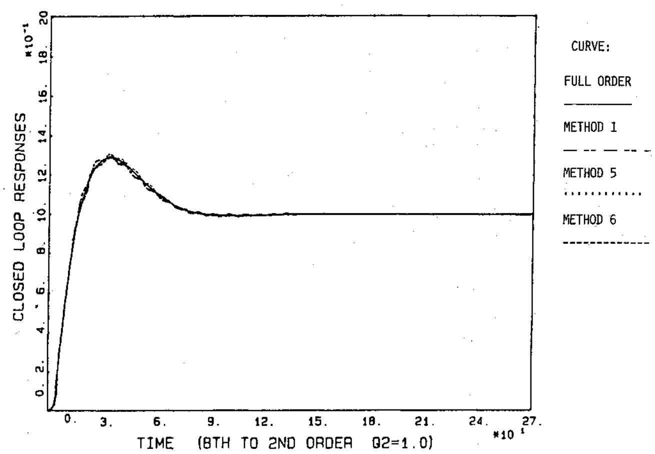

Fig. 1b **Comparison of unit step responses of second-order compensators given by methods 1, 5, and 6 with full-order design (small q_2).**

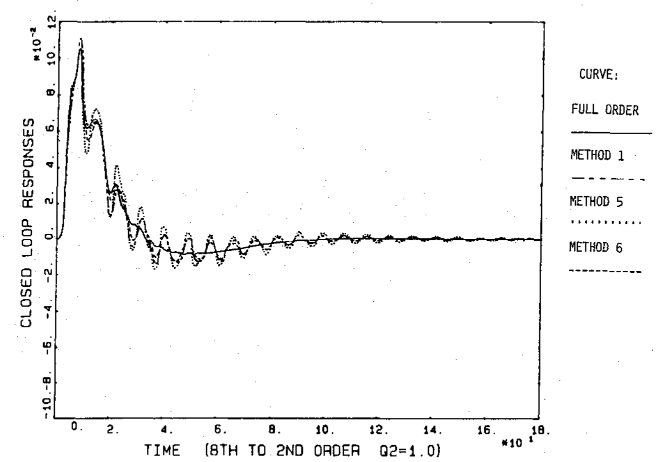

Fig. 2b **Comparison of impulse responses of second-order compensators given by methods 1, 5, and 6 with full-order design (small q_2).**

sponse. This agreement is slightly exceeded by method 6 (Fig. 2b), but on the whole, methods 1, 5, and 6 show excellent performance.

On the other hand, for a fairly large value of q_2, both stability and agreement with LQG response is degraded somewhat for several methods. Figures 3 and 4 show comparisons of unit step and impulse responses for the case $N_c = 5$ and $q_2 = 100$. In this case, only methods 1, 3, 5, and 6 yield stable designs and are thus compared. Of the LQG reduction methods, method 5 exhibits distinctly better agreement with the LQG responses. Once again, it is found (Figs. 3b and 4b) that method 6 somewhat excels in the accuracy with which its transient responses track the full-order design.

Thus, for the 42 design cases studied in this example problem, methods 1 and 5 demonstrate good success in achieving stable closed-loop designs while method 6 achieves stable designs in all cases.

Also, in the cases examined, methods 1 and 5 offer good transient response characteristics while method 6 tracks the full-order compensator response the closest.

In view of the good performance exhibited by method 6, we present, in the remainder of this section, additional details on the OP design results and the performance of the solution algorithm described in Sec. III.

First, as noted, the OP design philosophy focuses on the steady-state quadratic performance index J (defined in Sec. III) as the "figure of merit" for a reduced-order compensator design. Thus, we appropriately display, in Fig. 5, several plots of the performance index J (normalized by q_2) versus compensator order for all seven values of q_2. Note that apart from minor variations that are likely due to the benign convergence tolerance used in the solution algorithm, J generally decreases monotonically with increasing N_c. These graphs thus illustrate the basic trade-off between performance and controller complexity.

Note that for small q_2 (Fig. 5a), performance is not much affected by order reduction. This is to be expected since small disturbance noise intensity, in this problem, leads to low observer gains and to small values for the terms involving $\tau_\perp$ in Eqs. (10a–10e). Since the $\tau_\perp$ terms in Eqs. (10a–10e) have little effect, the OP designs are approximated by balanced projections of the LQG design. This might also help to explain the relatively successful performance of all methods for small q_2.

For large values (Fig. 5b) and for very large values (Fig. 5c) of q_2, however, the degradation of performance with reduction in order is increasingly steep. For example, although for $q_2 = 1.0$, the second-order performance is only 2.5% above the LQG performance, for $q_2 = 2000$, the second-order performance is 270% above the LQG value. Thus, order reduction under large disturbance noise does appear to be a more delicate matter.

While increasing difficulties with q_2 are not clearly manifested in the stability or transient response properties of the OP designs, these are reflected in the computation required to arrive at the final designs.

To explain this, we now describe the specific design steps taken and the performance of the solution algorithm. Each design case was treated using the OP solution algorithm discussed in Sec. III and a maximum homotopy step size of 1.0 was input. Furthermore, for each design case, the algorithm

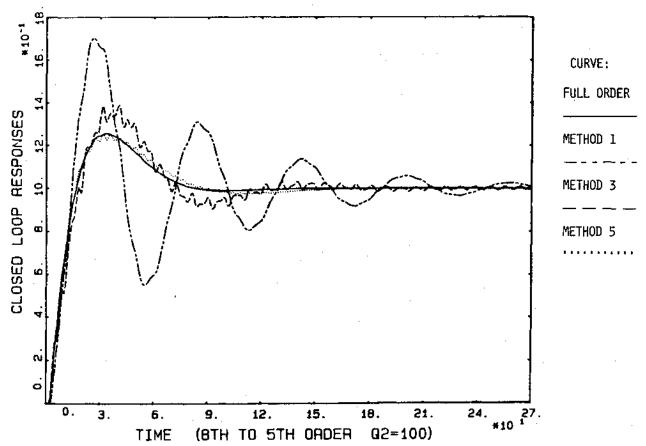

Fig. 3a Comparison of unit step responses of fifth-order compensators given by methods 1, 3, and 5 with full-order design (large q_2).

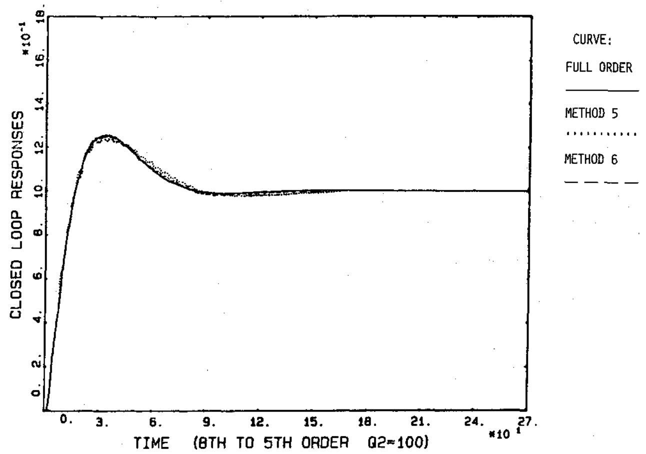

Fig. 3b Comparison of unit step responses of fifth-order compensators given by methods 5 and 6 with full-order design (large q_2).

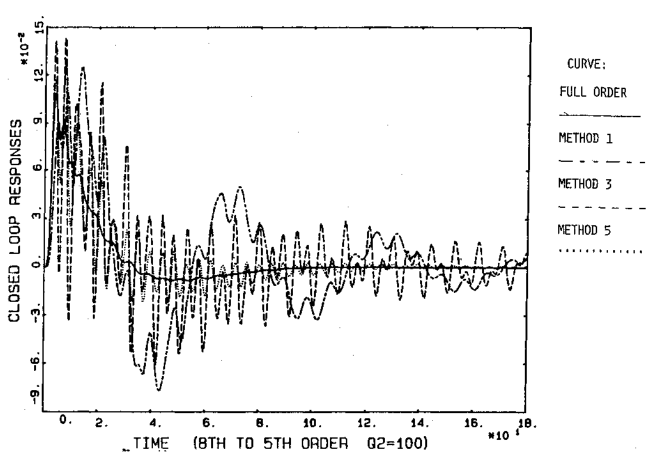

Fig. 4a Comparison of impulse responses of fifth-order compensators given by methods 1, 3, and 5 with full-order design (large q_2).

was started "cold," i.e., without being initialized with gain values obtained in previous cases. On initial application of the algorithm, the OP design results presented here were obtained after using the number of inner loop iterations given for each case in Table 4.

Note that with $\Delta = 1.0$, the logic of the outer loop implies a minimum of two inner-loop iterations. Inspection of the results obtained in some of the benign cases suggested the possibility that only one inner loop iteration was needed. Consequently

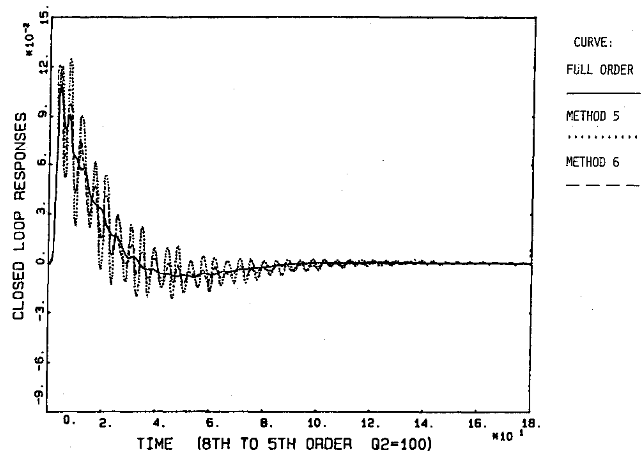

Fig. 4b Comparison of impulse responses of fifth-order compensators given by methods 5 and 6 with full-order design (large q_2).

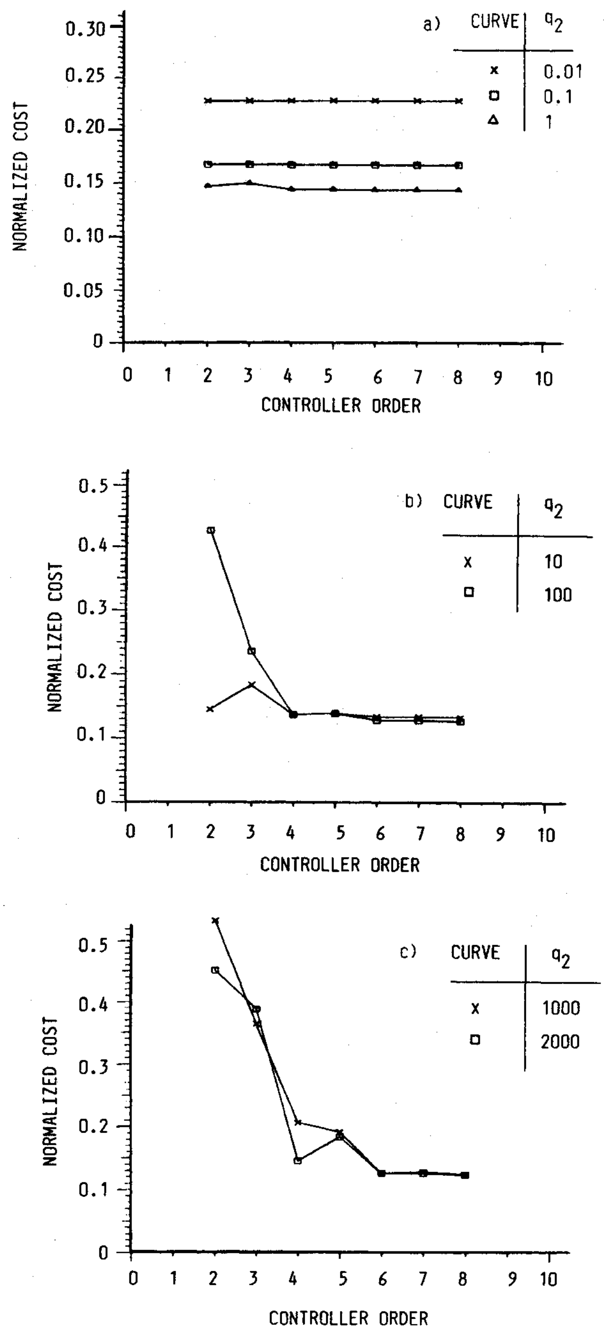

Fig. 5 Steady-state quadratic performance of OP designs vs compensator order for all values of q_2.

Table 4 Number of inner-loop iterations used in OP solution algorithm—initial design computations

Order, N_c \ q_2	0.01	0.1	1	10	100	1000	2000
7	2	2	2	4	5	8	10
6	2	2	2	6	4	8	10
5	2	2	2	6	5	5	7
4	2	2	2	8	9	6	10
3	4	4	4	8	9	7	8
2	4	4	4	8	9	9	10

we re-examined the cases comprising $q_2 = 0.01$, 0.1, and 1.0 and $N_c = 5$, 6, and 7 by revising the outer loop logic to output gain values after only one pass through the inner loop. It was found that this produced acceptable accuracy in the cases $q_2 = 0.01$; $N_c = 5$, 6, 7; $q_2 = 0.1$; $N_c = 6$, 7; and $q_2 = 1.0$; $N_c = 7$.

At the time of writing, full compilation of the computation times required for all methods on the same machine is not available. All OP calculations were performed on a Harris H800 minicomputer. However, as a rough estimate, it is fair to say that in the benign cases the OP computation is comparable to the burden incurred by methods 1–5. For the difficult, large q_2 cases, the OP computational burden is clearly in excess of methods 1–5 (although certainly not excessive from a practical point of view). However, it is precisely in these cases that the LQG reduction methods experience the greatest difficulties in producing closed-loop stable designs. Thus a meaningful comparison of relative computational burden in these cases cannot be performed.

Finally, it should be noted that the computational burden associated with OP for the designs presented here is also an artifact of the solution algorithm described in Sec. III and is not solely the result of the design equations themselves. This algorithm was convenient to use and was the first implemented since it requires only standard LQG software. On the other hand, this algorithm takes no particular advantage of the special structure of the fundamental design Eqs. (10a–10e). Its principal drawback is that it involves the iterative solution of four NxN, nonlinear matrix equations. To remedy this, Richter[12] has developed a step-wise homotopy algorithm which requires, at each homotopy step, the solution of four N_cxN linear equations. Clearly, for small N_c, this offers the potential for computing an OP design with less computational burden than is required for a full-order LQG design. It is anticipated that the future use of Richter's algorithm will permit a more accurate and definitive comparison between the computational cost of the LQG-reduction techniques and the Optimal Projection formulation.

V. Conclusions

In this paper, we have used an eighth-order example problem to perform a computational comparison of six methods for reduced-order dynamic compensator design. Methods 1–5 are based upon linear-quadratic reduction procedures while method 6 is based upon the Optimal Projection formulation.

Of the linear-quadratic reduction methods, the frequency-weighted balancing method of Enns and a recent method of Liu and Anderson exhibited particularly good stability and transient response properties. However, in the cases examined, the Optimal Projection method gave somewhat better transient response characteristics and, unlike the linear-quadratic reduction procedures, produced closed-loop stable designs for all the 42 design cases.

A precise comparison of the computational burdens incurred by the various methods is not possible at present. However, as a rough comparison, it is fair to say that the Optimal Projection method entailed comparable computation in the relatively benign design cases and more computation in the difficult cases. However, in this case, linear-quadratic reduction methods often produce unstable designs. Thus the Optimal Projection method exhibits a trade-off between computational burden and corresponding design reliability. Current developments are directed toward implementing advanced homotopy techniques that take particular advantage of the structure of the basic Optimal Projection design equations to markedly improve design computation speed.

Appendix

In the following, numerical values of the reduced-order compensator gains K, F, and A_c obtained via the OP solution algorithm discussed in Sec. III are given for the design cases: $q_2 = 2000$ and $N_c = 2$, 3, 4, and $N_c = 2$ and $q_2 = 0.01$, 0.1, 1.0, 10, 100, 1000.

Case: $q_2 = 2000$, $N_c = 4$

$$A_c = \begin{bmatrix} 0.3225E-02 & -0.3717 & 0.1238E-01 & -0.5735E-01 \\ 2.170 & -0.3860E-02 & -0.3623 & -0.1829E-01 \\ -0.1140 & 0.5365 & -0.2564E-01 & -0.2749 \\ 1.176 & -0.1297 & 0.3488 & -0.4452 \end{bmatrix}$$

$$F^T = [\ 0.9245E-04 \quad 0.6044E-01 \quad -0.3234E-02 \quad 0.3370E-01]$$

$$K = [-0.4871 \quad 0.5626 \quad 0.6852 \quad 2.540]$$

Case: $q_2 = 2000$, $N_c = 3$

$$A_c = \begin{bmatrix} 0.2351E-02 & 0.1516 & 0.1492 \\ -1.447 & -0.9385E-01 & 0.6597 \\ -1.592 & -0.7041 & -0.1027E-02 \end{bmatrix}$$

$$F^T = [\ 0.5944E-04 \quad -0.3619E-01 \quad -0.3990E-01]$$

$$K = [-0.5372 \quad -1.410 \quad 0.1033]$$

Case: $q_2 = 2000$, $N_c = 2$

$$A_c = \begin{bmatrix} -0.8378E-03 & -0.4671 \\ 2.047 & -0.1095E-01 \end{bmatrix}$$

$$F^T = [\ 0.3272E-04 \quad -0.7625E-01]$$

$$K = [\ 0.3807 \quad -0.6411]$$

Case: $q_2 = 1000$, $N_c = 2$

$$A_c = \begin{bmatrix} 0.1745E-02 & 0.4039 \\ -2.129 & -0.7569E-02 \end{bmatrix}$$

$$F^T = [-0.6242E-04 \quad 0.7341E-01]$$

$$K = [\ 0.3753 \quad 0.5049]$$

Case: $q_2 = 100, \quad N_c = 2$

$$A_c = \begin{bmatrix} 0.2742E-02 & 0.4216 \\ -2.396 & -0.2274E-01 \end{bmatrix}$$

$$F^T = [-0.1538E-03 \quad 0.1303]$$

$$K = [\ 0.2351 \quad 0.4178]$$

Case: $q_2 = 10, \quad N_c = 2$

$$A_c = \begin{bmatrix} 0.7474E-02 & 0.1970 \\ -1.699 & -0.8276 \end{bmatrix}$$

$$F^T = [\ 0.4814E-03 \quad -0.1081]$$

$$K = [-0.1740 \quad -0.9190]$$

Case: $q_2 = 1, \quad N_c = 2$

$$A_c = \begin{bmatrix} 0.7832E-02 & -0.1812 \\ 1.269 & -0.7143 \end{bmatrix}$$

$$F^T = [\ 0.8516E-03 \quad 0.1356]$$

$$K = [-0.1003 \quad 0.5206]$$

Case: $q_2 = 0.1, \quad N_c = 2$

$$A_c = \begin{bmatrix} 0.9915E-02 & -0.1578 \\ 0.7650 & -0.5093 \end{bmatrix}$$

$$F^T = [\ 0.1695E-02 \quad 0.1264]$$

$$K = [\ -0.5729E-01 \quad 0.2733]$$

Case: $q_2 = 0.01, \quad N_c = 2$

$$A_c = \begin{bmatrix} 0.1357E-01 & -0.1398 \\ 0.3985 & -0.3430 \end{bmatrix}$$

$$F^T = [0.3451E-02 \quad 0.9371E-01]$$

$$K = [0.3045E-01 \quad 0.1421]$$

Acknowledgment

This research was supported in part by the Air Force Office of Scientific Research, Contract AFOSR F49620-86-C-0038.

References

[1]Liu, Y. and Anderson, B. D. O., "Controller Reduction Via Stable Factorization and Balancing," *International Journal of Control*, Vol. 44, No. 2, 1986, pp. 507–531.

[2]Enns, D., "Model Reduction for Control System Design," Ph.D. Dissertation, Stanford Univ., Palo Alto, CA, 1984.

[3]Glover, H., "All Optical Hankel-Norm Approximations of Linear Multivariable Systems and Their L-Error Bounds," *International Journal of Control*, Vol. 39, 1984, p. 1115.

[4]Davis, J. A. and Skelton, R. E., "Another Balanced Controller Reduction Algorithm," *System Control Lett.*, Vol. 4, 1984, p. 79.

[5]Yousuff, A. and Skelton, R. E., "A Note on Balanced Controller Reduction," *IEEE Transactions on Automatic Control*, Vol. 29, 1984, p. 254.

[6]Hyland, D. C. and Bernstein, D. S., "The Optimal Projection Equations for Fixed-Order Dynamic Compensation," *IEEE Transactions on Automatic Control*, Vol. AC–29, 1984, pp. 1034–1037.

[7]Hyland, D. C., "Comparison of Various Controller-Reduction Methods: Suboptimal Versus Optimal Projection," *Proceedings AIAA Dynamics Specialists Conference*, Palm Springs, CA, May 1984, pp. 381–389.

[8]Bernstein, D. S. and Hyland, D. C., "The Optimal Projection Equations for Finite-Dimensional Fixed-Order Dynamic Compensation of Infinite-Dimensional Systems," *SIAM Journal of Control and Optimization*, Vol. 24, 1986, pp. 122–151.

[9]Rao, C. R. and Mitra, S. K., *Generalized Inverse of Matrices and Its Applications*, Wiley, New York, 1971.

[10]Kato, T., *Perturbation Theory for Linear Operators*, Springer-Verlag, New York, 1966.

[11]Hyland, D. C. and Bernstein, D. S., "The Optimal Projection Equations for Model Reduction and the Relationships Among the Methods of Wilson, Skelton, and Moore," *IEEE Transactions on Automatic Control,* Vol. AC-30, 1985, pp. 1201–1211.

[12]Richter, S., "A Homotopy Algorithm for Solving the Optimal Projection Equations for Fixed-Order Dynamic Compensation: Existence, Convergence, and Global Optimality," *American Control Conference*, Minneapolis, MN, June 1987, pp. 1527–1531.